The Muon $g-2$ experiment at Fermilab

James Mott

On behalf of the Muon $g-2$ experiment

Received: July 31, 2018

Abstract Precision measurements of the anomalous magnetic moment of the muon a_μ are a stringent test of the Standard Model. The last measurement of a_μ at Brookhaven National Laboratory (BNL) differs from the Standard Model prediction by 3-4σ: a possible indication of new physics. A successor to that experiment has been constructed at Fermilab, with the aim of reducing the experimental uncertainty by a factor of four to 140 ppb. The measurement technique continues to use the storage ring concept from BNL, with muons circulating in a highly uniform magnetic dipole field. The spin precession frequency is extracted by analysing the modulation of the rate of higher-energy positrons from muon decays, which are detected by 24 calorimeters around the inside of the ring. Compared to the previous experiment, significant improvements have been made in the areas of muon beam preparation, storage ring hardware, field measuring equipment, and detector and electronics systems. In these proceedings, I report on the status of the experiment as of June 2018, presenting an overview of the experiment's progress, some initial data from the first run, and the anticipated timeline for a new result.

1 Introduction

The muon anomaly, $a_\mu \equiv (g_\mu - 2)/2$, is an interesting quantity as it can be both measured and predicted to a high level of accuracy. For spin-$\frac{1}{2}$ Dirac fermions a_μ is 0, but in reality contributions from virtual loops mean the value is non-zero. A stringent test for the presence of new physics is therefore to compare the theoretical prediction with an experimental measurement, which may differ due to effects from loops containing as yet unknown particles. Currently the best experimental measurement comes from this experiment's predecessor at BNL. The final result of $a_\mu = 116\,592\,089\,(54)\text{st}\,(33)\text{sy}\,(63)\text{tot} \times 10^{-11}$ [1] leads to a discrepancy between experiment and theory at the level of $\Delta a_\mu = [269 \pm 72] \times 10^{-11}$ or 3.7σ [2]. This compelling difference provides motivation for the Muon $g-2$ experiment at

James Mott
Boston University, Boston, MA 02215, U.S.A
E-mail: jmott@bu.edu

Fermilab, which will measure a_μ with 21 times higher statistics and a reduction in systematic uncertainty by a factor 2-3 compared to the BNL experiment. If both experimental and theoretical central values remain unchanged, then the combined reduction in uncertainties would lead to a discrepancy at the level of 7.5σ (or 5σ with experimental improvements alone).

2 Muon $g-2$ experiment at Fermilab

The Muon $g-2$ experiment at Fermilab employs similar experimental principles to the BNL experiment [3]. Longitudinally-polarised muons are injected into a storage ring with a highly uniform magnetic dipole field. A measurement of a_μ is obtained by measuring the magnetic field averaged over the muon distribution, B, and the anomalous precession frequency, ω_a. On an ideal orbit, with a perfectly uniform magnetic field, these are related by:

$$\omega_a = \omega_s - \omega_c = \frac{e}{mc}\left[a_\mu B - \left(a_\mu - \frac{1}{\gamma^2-1}\right)\boldsymbol{\beta}\times\mathbf{E} - a_\mu\left(\frac{\gamma}{\gamma+1}\right)(\boldsymbol{\beta}\cdot\mathbf{B})\boldsymbol{\beta}\right] \quad (1)$$

where ω_s is the spin precession frequency of the muons in the magnetic field and ω_c is their cyclotron frequency. The second term is a result of the boost of electric focusing fields present in the laboratory to the muon rest frame and vanishes for muons stored at the magic momentum of 3.09 GeV. The third term enters if the motion of the muon is not perpendicular to the magnetic field such that $\boldsymbol{\beta}\cdot\mathbf{B}$ is non-zero. In reality, stored muons have a small momentum spread around the magic momentum and also have some small degree of vertical motion. The momentum spread and vertical motion are extracted from the data and the two resulting sub-ppm corrections are made to the measured precession frequency.

The muon storage ring from BNL is being reused in the Fermilab experiment (see Section 3). Its superconducting coils were transported from BNL to Fermilab in a high-profile move in 2013. Magnet re-assembly and commissioning in a newly constructed experimental hall at Fermilab's "Muon Campus" began in mid-2014. Full field strength was reached in Sep. 2015, allowing for the start of a campaign to improve field uniformity with field shimming.

After shimming, the vacuum chambers, muon storage systems, calorimeter and tracker systems were installed, with the process completed by mid-2017 (see Section 4). Around the same time, the majority of modifications to the Fermilab accelerator complex were finished, and the first beam entered the storage ring in Jun. 2017. A one-month engineering run was completed, providing enough data for proof-of-principle of operation of all systems.

The outstanding changes to the incoming beamlines were made by Nov. 2017, after which the complex provides a high-purity (π fraction $< 10^{-5}$), intense (8×10^6 μ^+/sec) beam of $\sim 96\%$ longitudinally-polarised μ^+ to the experimental hall. After optimisation of the incoming beam and storage ring hardware, the experiment started collecting production data in Mar. 2018. A preliminary online estimate of the number of higher-energy positrons detected at the calorimeters by mid-May 2018 is shown in Figure 1. By way of comparison, the BNL experiment collected a total of 10^{10} higher-energy positrons.

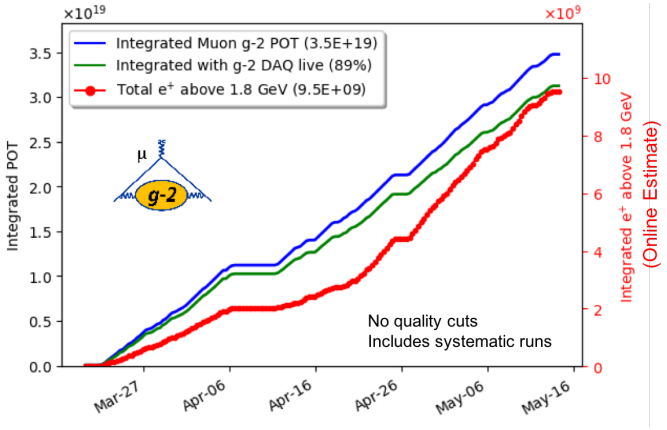

Fig. 1 Online estimate of the number of positrons above 1.8 GeV collected during Run 1 as of mid-May 2018. This reported number is before any quality cuts and includes systematic test runs.

3 Magnetic Field

The storage magnet is the same one used in the BNL experiment. It is a 14 m diameter toroidal C-shaped magnet, comprising 12 iron yokes and superconducting coils carrying 5.2 kA, thus providing a 1.45 T vertical dipole magnetic field. A section through the magnet is shown in Figure 2.

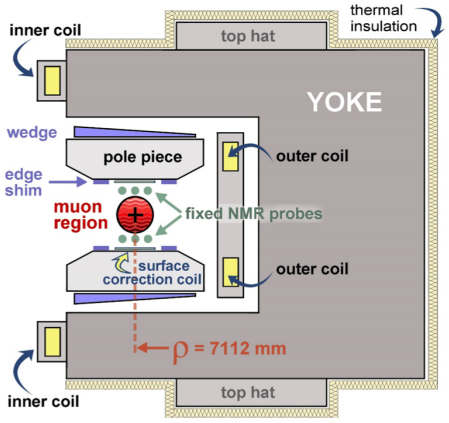

Fig. 2 Cross section through C-shaped storage ring magnet. Current flows between inner and outer coils inducing a vertical dipole field between the pole pieces.

A measurement of the magnetic field strength is one of two ingredients that determine the value of a_μ. The field in the storage region is periodically measured with a trolley containing 17 proton NMR probes that rides on a set of rails inside the vacuum chamber. Between these runs, the field is monitored using pulsed proton NMR with 400 fixed probes located above and below the muon storage volume.

Absolute field probes are used to translate from the proton Larmor precession frequency of the NMR probes to an absolute magnetic field value. These probes are cross-calibrated against the one used in the muonium hyperfine experiment from which the muon-to-proton magnetic moment ratio is drawn [4], reducing another source of potential systematic uncertainty in the extraction of a_μ [3].

The specific value required to extract a_μ is the magnetic field convoluted with the spatial distribution of stored muons. In order to reduce the requirement on the knowledge of the muon distribution, the magnetic field is made as uniform as possible. The specifications are ± 25 ppm for point-to-point variations and < 1 ppm when averaged azimuthally around the ring. The magnet has many calibration handles for improving field uniformity, as detailed in Figure 2. The location and orientation of these magnetic components affects the field strength and direction in localised regions of the ring. 72 high-purity iron pole pieces and 48 iron top hats are used to make coarse changes to the vertical dipole field and 864 iron wedges and 144 edge shims are deployed to reduce any quadrupole or sextupole asymmetries. At a finer level, 8000 thin iron foils are attached to the surface of the poles providing very localised modifications of overall field strength. The combination of these passive shimming pieces are intended to account for small ($<$100 µm) alignment errors and intrinsic magnetic material variation.

An iterative shimming procedure was completed in Aug. 2016. The dipole field uniformity at the beginning and end of the process can be seen in Figure 3. At the start, the field variation was at the level of 1400 ppm with a repeating structure from misaligned pole pieces. After shimming, the field is much more uniform, lying within the ± 25 ppm point-to-point target.

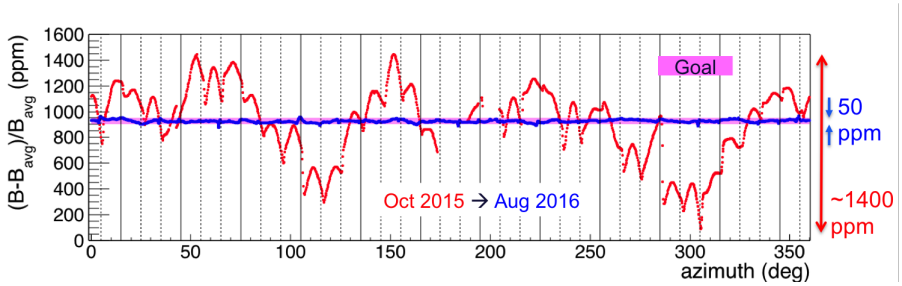

Fig. 3 Magnetic dipole field in the storage ring before (red) and after (blue) shimming. The blue line lies within the magenta band confirming that the target uniformity has been reached.

The target is to reduce the systematic uncertainty from the magnetic field measurement from 170 ppb at BNL to 70 pbb with this experiment. For the most part, an acceptable level can be reached by small improvements rather than drastic changes. These small improvements include better knowledge of the NMR trolley location, reduced trolley temperature changes, better temperature control in the experimental hall, a larger number of viable fixed NMR probes, and digitisation of the full probe waveforms to enable measurements in regions of higher field gradients.

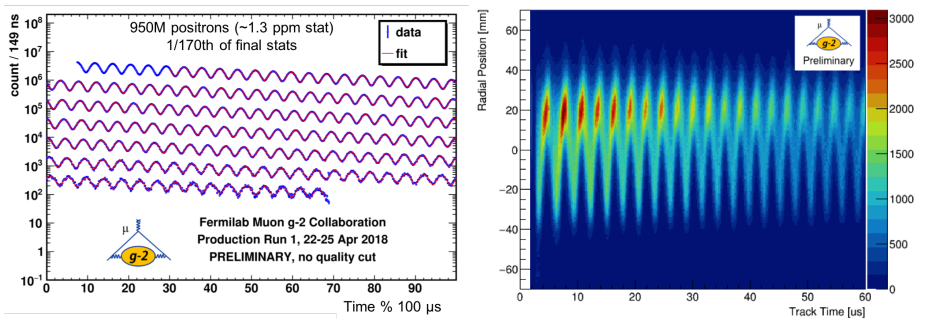

(a) (b)

Fig. 4 (a) Oscillation in arrival times of high-energy positrons due to spin precession from 60h of data from Run 1. (b) Estimated radial position of muon decay from extrapolated positron tracks vs. time. The beam oscillates radially due to betatron oscillations from both a weak kick and a phase space mismatch during injection into the ring.

4 Detector Systems

A measurement of ω_a is the second element required to extract a_μ. The spin precession frequency is accessible due to parity violation in $\mu^+ \rightarrow e^+\bar{\nu}_\mu\nu_e$ decay. Higher-energy positrons are preferentially emitted along the direction of the muon spin, so as the spin direction oscillates radially inwards and outwards the number of higher-energy positrons is modulated at the same frequency. There are 24 calorimeters located on the inside of the storage ring that determine the arrival time and energy of decay positrons. If an energy threshold is applied to the detected positrons, then the oscillation in detection rate due to the spin precession appears, as shown in Figure 4a. This plot contains 950M higher-energy positrons collected over a few days in Apr. 2018, and would correspond to a statistical uncertainty of 1.3 ppm.

Every calorimeter contains an array of 6×9 PbF_2 crystals, each read out by a SiPM and digitised at 800 MSPS with 12-bit resolution by custom frontend boards [5]. Pile-up is one of the largest sources of systematic error, since two low-energy positrons arriving at a similar time can be mistaken for one higher-energy positron. The pile-up rate changes as muons decay and so these misidentifications introduce a time-dependent effect that can directly impact the ω_a measurement. The segmented calorimeter allows for spatial separation of positrons and the fast response of the crystals coupled with the high frequency digitisation of the waveform allow temporal separation at the 4 ns level. The gain stability of the calorimeter over the course of each fill of the ring is also very important as the measurement relies on selecting positrons above a given threshold. To cross-check this stability, a laser calibration system has been developed which introduces laser pulses in one out of every ten storage ring fills and additional out-of-fill pulses during the measurement period. This system provides gain stability at a level better than 1 part in 10^4 per hour [5,6].

Additionally, within the vacuum chamber in front of two of the calorimeters, there are two straw trackers for measuring positron tracks which can be extrapolated backwards to infer the point of muon decay. Each tracker comprises eight

modules with 32 layers of straws for a total of 2000 straws. The trackers' main role is to extract the spatial profile of the stored muons. This is used to appropriately weight the magnetic field measurements and to ascertain the values of the two corrections to ω_a in Equation 1. Figure 4b shows the measured radial position of the beam as a function of time using extrapolated tracks. The observed radial oscillation of the beam is a result of betatron oscillations due to the unavoidable phase space mismatch between the incoming beam and the storage ring. In addition to beam measurements, the trackers provide independent time and momentum measurements of positrons that can be used to cross-check the calorimeter efficiency and gain, and to test pile-up identification techniques.

5 Outlook

The first run of the Muon $g-2$ experiment at Fermilab has been a success. Projecting from Figure 1, we expect to comfortably collect enough positrons during this run to produce a result with improved precision compared to the BNL measurement. We anticipate that this result will be ready for publication in 2019. Data collection will continue for two more years with the complete dataset (containing more than 20 times the BNL statistics) expected by 2020. An intermediate measurement with a precision of 200 ppb is planned for 2020 and a final result should be available by 2022. In addition to the a_μ value, we anticipate additional results of a search for a muon EDM and tests for Lorentz violation in at least two of the datasets.

This work was supported in part by Fermilab and the US DOE Office of High Energy Physics.

References

1. G.W. Bennett et al., Final Report of the Muon E821 Anomalous Magnetic Moment Measurement at BNL, Phys. Rev. D73 072003 (2006)
2. A. Keshavarzi et al., Muon $g-2$ and $\alpha(M_Z^2)$: A new data-based analysis, Phys. Rev. D97 114025 (2018)
3. J. Grange et al., Muon (g-2) Technical Design Report, arXiv:1501.06858 [physics.ins-det] (2015)
4. W. Liu et al., High precision measurements of the ground state hyperfine structure interval of muonium and of the muon magnetic moment, Phys. Rev. Lett. 82 711714 (1999)
5. A.T. Fienberg et al., Studies of an array of PbF_2 Cherenkov crystals with large-area SiPM readout, Nucl. Instrum. Meth. A783 1221 (2015)
6. A. Anastasi et al., Test of candidate light distributors for the Muon $g-2$ laser calibration system, Nucl. Instrum. Meth. A788 4348 (2015)